GEOPHYSICS, VOL. 57, NO. 9 (SEPTEMBER 1992), P. 1166–1177, 12 FIGS.

Adaptive surface-related multiple elimination

D. J. Verschuur*, A. J. Berkhout*, and C. P. A. Wapenaar*

ABSTRACT

The major amount of multiple energy in seismic data is related to the large reflectivity of the surface. A method is proposed for the elimination of all surface-related multiples by means of a process that removes the influence of the surface reflectivity from the data. An important property of the proposed multiple elimination process is that no knowledge of the subsurface is required. On the other hand, the source signature and the surface reflectivity do need to be provided. As a consequence, the proposed process has been implemented adaptively, meaning that multiple elimination is designed as an inversion process where the source and surface reflectivity properties are estimated and where the multiple-free data equals the inversion residue. Results on simulated data and field data show that the proposed multiple elimination process should be considered as one of the key inversion steps in stepwise seismic inversion.

INTRODUCTION

Many methods have already been developed to remove multiple reflections from the data. The most popular method is undoubtedly statistical least-squares, prediction-error filtering. It performs best on *small offset* reflection data from one-dimensional (1-D) media. Multiple elimination based on velocity discrimination (CMP stacking, optionally preceded by filtering in the *f-k* or τ-p domain) assumes that the primaries and multiples have sufficient differential moveout to make a distinction between them. Still a human interpretation of the data is needed to make this distinction, if at all possible, and the method performs best on *large offset* data. An important category of model-based multiple elimination methods removes all water-layer multiples and water layer reverberations by wave theory-based prediction. A model of the water *layer* must be available.

The proposed surface-related multiple elimination method appears to be a very attractive alternative, especially in those situations where the above methods fail, e.g., in situations with small or difficult-to-distinguish velocity differences between primaries and multiples, or in complex media where such simple methods do not suffice. In the case of strong subbottom reflectors, relatively strong surface-related multiples (which are not all water layer-related) can be expected in the data, particularly for a deep target (say later than 2 s). In this situation, the surface-related multiple elimination looks very promising.

The historical development of this method starts with Anstey and Newman (1967), who observed that with the autoconvolution of a trace, primary events were transformed into multiples. Kennett (1979) described an inversion scheme in the k_x-ω domain to eliminate multiples for a horizontally layered elastic medium. Berkhout (1982, chapter 7) redefined the multiple problem for laterally varying media by using a wave theory-based matrix formulation. An adaptive version has been shown with examples in Verschuur et al. (1989) and Wapenaar et al. (1990). The method described here is based on Berkhout's approach and handles both single-component acoustic and multicomponent elastic data. In the latter case, by taking the full elastic reflection at the free surface into account, all surface-related multiply reflected and converted events can be eliminated. In all cases, it is important that the data represent upgoing reflected waves, related to downgoing source waves. Hence, before applying this multiple elimination procedure, a decomposition of the measured seismic data into up- and downgoing waves must be applied (preprocessing). In this paper, we will concentrate on the marine case.

The proposed method can be considered as the counterpart of the wave equation-based water layer, multiple prediction method, as described in Bernth and Sonneland (1983), Berryhill and Kim (1986), and Wiggins (1988). In these methods, the wavefield is extrapolated one round trip through the water layer, so that each event is transformed into a water-layer-related multiple of one order higher than it is. These predicted multiples are then adaptively subtracted from the data.

Manuscript received by the Editor April 1, 1991; revised manuscript received January 14, 1992.
*Laboratory of Seismics and Acoustics, Delft University of Technology, P. O. Box 5046, 2600 GA Delft, The Netherlands.

When comparing published techniques with our scheme, the following differences are found:

1) The parameters for our adaptive procedure are significantly simpler: i.e., surface *boundary* parameters versus surface *layer* parameters.
2) The number of types of multiples that are eliminated in our procedure is larger: i.e., all surface-related multiples versus the water-layer-related multiples. This advantage becomes more noticeable deeper in the seismic section.

On principle, the multiple elimination method as described in this paper can be applied in a three-dimensional (3-D) sense. From a theoretical point of view, this requires seismic data to be measured on a dense grid in the x- and y-direction, for both sources and receivers. However, it may be expected that this strict theoretical requirement can be relaxed. This important aspect is being studied now. In this paper, only the two-dimensional (2-D) case will be considered.

MULTIPLE ELIMINATION FOR SINGLE-COMPONENT DATA

Forward model of seismic data

The multiple elimination procedure can be expressed for data acquired in both acoustic and elastic media. The derivation for the single-component case will be given here, assuming that only longitudinal (P) waves are measured. For marine data this is always the case, as acquisition is done in the water layer. For land data, the theory requires multicomponent data. However, experiments on synthetic land data show that good results are also obtained for single-component data. In fact, the proposed method can be formulated as a well-stabilized inversion process and therefore a forward model of the seismic data will be derived first. The matrix notation introduced in Berkhout (1982) will be used.

We consider a 2-D seismic line with a fixed spread of N detectors. The shot is positioned at the first detector position and moved one detector spacing after each shot, finally resulting in N shot records, as shown in Figure 1. The shot records are Fourier transformed to the frequency domain, and data are separated for each frequency. This results in N monochromatic common-shot gathers, each consisting of N complex samples. These monochromatic shot records are stored into the columns of a matrix, defining the data matrix for this particular frequency. Such a data matrix can be constructed for each frequency component. So one data matrix describes the total 2-D seismic data for one frequency component. As most seismic processing can be done independently for each frequency, this matrix notation is very powerful. Matrices are indicated with bold capitals and a tilde underneath, like $\utilde{\mathbf{P}}^-(z_0)$, in which z_0 indicates the depth level $z = z_0$ to which this matrix is related (i.e., the depth level at which source and receivers are located). For 2-D seismic data, we get matrices of dimension N with the zero offset data on the main diagonal and the common-midpoint data on the antidiagonals. With this discretized notation, spatial convolutions can be described by matrix multiplications. Note that in practice, the defined square data matrices are only partly filled with data (i.e., a band matrix).

The upgoing pressure wavefield $\utilde{\mathbf{P}}_0^-(z_0)$ at the surface can be written as:

$$\utilde{\mathbf{P}}_0^-(z_0) = \utilde{\mathbf{X}}_0(z_0, z_0)\utilde{\mathbf{S}}^+(z_0), \tag{1}$$

where $\utilde{\mathbf{S}}^+(z_0)$ is the matrix containing the downgoing source wavefields at the surface and $\utilde{\mathbf{X}}_0(z_0, z_0)$ is the response matrix of the subsurface for a *nonreflecting* surface. $\utilde{\mathbf{X}}_0(z_0, z_0)$ contains all primary reflections and *internal* multiples of the subsurface. The reference z_0 indicates that the data is related to the surface. Figure 2a gives schematically the model of the seismic data as defined in equation (1). Note that the upgoing wavefield as given in equation (1) is not directly the measured seismic data. We will come back to that later. Note also that the description of equation (1) is a multisource description, as each column in the source matrix $\utilde{\mathbf{S}}^+(z_0)$ contains the downgoing source wavefield for each

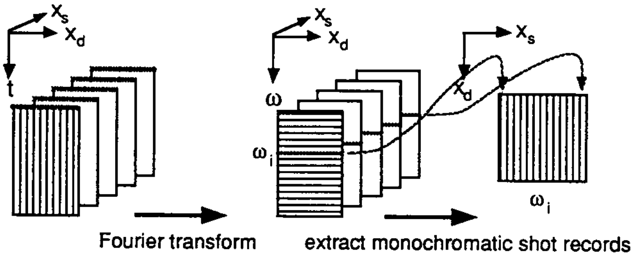

FIG. 1. A full data matrix is acquired with a fixed spread of detectors and the source positioned at a detector position for each shot record experiment. The detector positions for one shot record correspond with the elements of one column in the data matrix. The shot records are first Fourier transformed to the frequency domain, then reordered into monochromatic shot records with each frequency component stored in a column of the monochromatic data matrix.

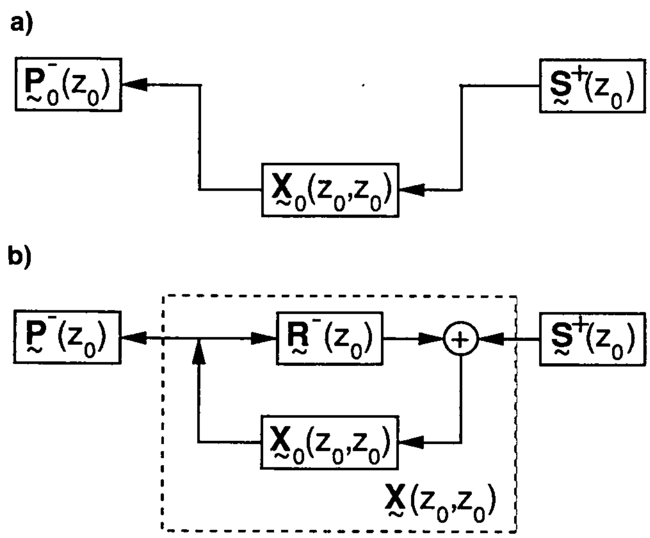

FIG. 2. (a) Forward model of seismic data without surface-related multiples. The source wavefield reflects in the subsurface and reflected waves arrive at the surface. (b) Forward model of seismic data with the surface-related multiples included. At the free surface the upgoing wavefields reflect and go back into the subsurface again.

shot record experiment. For pure dipole sources, the source matrix will be a diagonal matrix, with the diagonal elements being the source Fourier components $S_j(\omega)$, with j indicating the shot number. If source arrays are being used, the off-diagonal elements become nonzero, describing the array elements.

In the presence of a free surface, any upgoing wave arriving at the surface will reflect and transform into a downgoing wave. This means that the total downgoing wavefield leaving the surface not only consists of the illuminating source wavefield $\underline{\mathbf{S}}^+(z_0)$, but also of the downward reflected upgoing wavefield (including multiples), $\underline{\mathbf{R}}^-(z_0)$ $\underline{\mathbf{P}}^-(z_0)$. Hence, equation (1) should be modified according to

$$\underline{\mathbf{P}}^-(z_0) = \underline{\mathbf{X}}_0(z_0, z_0)[\underline{\mathbf{S}}^+(z_0) + \underline{\mathbf{R}}^-(z_0)\underline{\mathbf{P}}^-(z_0)], \quad (2)$$

with $\underline{\mathbf{P}}^-(z_0)$ being defined as the total upgoing wavefield at the surface z_0, and $\underline{\mathbf{R}}^-(z_0)$ being the reflectivity matrix of the free surface. Figure 2b gives the block diagram representation for equation (2) in which the reflecting surface effects have been included. Note that equation (2) is an implicit expression for the data with multiples $\underline{\mathbf{P}}^-(z_0)$. The explicit expression for the total upgoing wavefield at the surface including surface-related multiples can be derived from equation (2):

$$\underline{\mathbf{P}}^-(z_0) = [\underline{\mathbf{I}} - \underline{\mathbf{X}}_0(z_0, z_0)\underline{\mathbf{R}}^-(z_0)]^{-1}\underline{\mathbf{X}}_0(z_0, z_0)\underline{\mathbf{S}}^+(z_0), \quad (3a)$$

or, by defining $\underline{\mathbf{X}}(z_0, z_0)$ as the response of the subsurface with surface-related multiples included,

$$\underline{\mathbf{P}}^-(z_0) = \underline{\mathbf{X}}(z_0, z_0)\underline{\mathbf{S}}^+(z_0), \quad (3b)$$

with

$$\underline{\mathbf{X}}(z_0, z_0) = [\underline{\mathbf{I}} - \underline{\mathbf{X}}_0(z_0, z_0)\underline{\mathbf{R}}^-(z_0)]^{-1}\underline{\mathbf{X}}_0(z_0, z_0). \quad (3c)$$

The inverse matrix in equation (3a) can be expanded in a series, yielding

$$\underline{\mathbf{P}}^-(z_0) = \left[\sum_{n=0}^{\infty} \{\underline{\mathbf{X}}_0(z_0, z_0)\underline{\mathbf{R}}^-(z_0)\}^n\right]\underline{\mathbf{X}}_0(z_0, z_0)\underline{\mathbf{S}}^+(z_0), \quad (4a)$$

or,

$$\begin{aligned}\underline{\mathbf{P}}^-(z_0) = [\underline{\mathbf{I}} &+ \{\underline{\mathbf{X}}_0(z_0, z_0)\underline{\mathbf{R}}^-(z_0)\} \\ &+ \{\underline{\mathbf{X}}_0(z_0, z_0)\underline{\mathbf{R}}^-(z_0)\}^2 \\ &+ \{\underline{\mathbf{X}}_0(z_0, z_0)\underline{\mathbf{R}}^-(z_0)\}^3 \\ &+ \ldots]\underline{\mathbf{X}}_0(z_0, z_0)\underline{\mathbf{S}}^+(z_0). \quad (4b)\end{aligned}$$

Comparing equation (4) with equation (1) reveals that the extra terms in equation (4) generate all surface-related multiples.

For a pressure-free surface in the acoustic (marine) case, the reflectivity matrix $\underline{\mathbf{R}}^-(z_0)$ simplifies to:

$$\underline{\mathbf{R}}^-(z_0) = r_0\underline{\mathbf{I}}, \quad (5a)$$

in which ideally $r_0 = -1$. Taking the reflection matrix as a (scaled) unit matrix also requires that source and receiver positions are located on an equidistant grid. Strictly speaking, deviations from this requirement will give rise to (small) errors in the multiple elimination result. This can be overcome by including an interpolation operator in $\underline{\mathbf{R}}^-(z_0)$. However, we have noticed that our data-adaptive version can cope perfectly with this problem in a number of situations. For single-component land data, we do incorporate the full elastic reflectivity matrix $\underline{\mathbf{R}}^-(z_0)$ which describes reflection from P- to P-waves. As mentioned before, for single-component land data, we neglect S-waves.

Using equation (5a), equation (3a) simplifies to:

$$\underline{\mathbf{P}}^-(z_0) = [\underline{\mathbf{I}} - r_0\underline{\mathbf{X}}_0(z_0, z_0)]^{-1}\underline{\mathbf{X}}_0(z_0, z_0)\underline{\mathbf{S}}^+(z_0), \quad (5b)$$

or, by expanding the inversion term into a series:

$$\begin{aligned}\underline{\mathbf{P}}^-(z_0) = [\underline{\mathbf{I}} &+ r_0\underline{\mathbf{X}}_0(z_0, z_0) + r_0^2\underline{\mathbf{X}}_0^2(z_0, z_0) \\ &+ \ldots]\underline{\mathbf{X}}_0(z_0, z_0)\underline{\mathbf{S}}^+(z_0). \quad (5c)\end{aligned}$$

Note that $\underline{\mathbf{X}}_0(z_0, z_0)$ describes everything that happens in the subsurface, including elastic and even anisotropic effects and absorption. The *only* assumption made in equations (5a) to (5c) is that only P-waves are measured and that the surface reflectivity can be represented by reflection coefficient r_0. This is typically true for marine data.

Elimination of the surface-related multiples

To remove the multiples from the data $\underline{\mathbf{P}}^-(z_0)$, equation (2) can be inverted to get an explicit expression for $\underline{\mathbf{X}}_0(z_0, z_0)$:

$$\underline{\mathbf{X}}_0(z_0, z_0) = \underline{\mathbf{P}}^-(z_0)[\underline{\mathbf{S}}^+(z_0) + \underline{\mathbf{R}}^-(z_0)\underline{\mathbf{P}}^-(z_0)]^{-1}, \quad (6a)$$

or, by using equation (3b):

$$\underline{\mathbf{X}}_0(z_0, z_0) = \underline{\mathbf{X}}(z_0, z_0)[\underline{\mathbf{I}} + \underline{\mathbf{R}}^-(z_0)\underline{\mathbf{X}}(z_0, z_0)]^{-1}. \quad (6b)$$

Straightforward inversion of the inverse matrix at the right-hand side of equation (6b) results in instability if strong multiples are present. To understand this, the inverse matrix in equation (6b) is written as the following series expansion:

$$\underline{\mathbf{X}}_0(z_0) = \underline{\mathbf{X}}(z_0, z_0)\left[\sum_{n=0}^{\infty} \{-\underline{\mathbf{R}}^-(z_0)\underline{\mathbf{X}}(z_0, z_0)\}^n\right], \quad (7a)$$

or,

$$\begin{aligned}\underline{\mathbf{X}}_0(z_0, z_0) = \underline{\mathbf{X}}(z_0, z_0)[\underline{\mathbf{I}} &- \{\underline{\mathbf{R}}^-(z_0)\underline{\mathbf{X}}_0(z_0, z_0)\} \\ &+ \{\underline{\mathbf{R}}^-(z_0)\underline{\mathbf{X}}_0(z_0, z_0)\}^2 \\ &- \{\underline{\mathbf{R}}^-(z_0)\underline{\mathbf{X}}_0(z_0, z_0)\}^3 + \ldots]. \quad (7b)\end{aligned}$$

The inverse in equation (6b) implies an infinite number of terms at the right-hand side of equation (7). In the presence of strong multiple reflections (e.g., water reverberations at post-critical angles) the series expansion converges very slowly, and straightforward inversion as described by equation (6b) is unstable. Taking only a limited number of terms into account in equation (7) stabilizes the inversion. The number of terms that should be taken into account depends on the highest-order surface-related multiples present in the data (of finite duration), because each additional term taken into account in equation (7) results in eliminating surface-related multiples of one order higher.

Using equation (5a), equation (7b) becomes:

$$\mathbf{X}_0(z_0, z_0) = \mathbf{X}(z_0, z_0) - r_0\mathbf{X}^2(z_0, z_0) + r_0^2\mathbf{X}^3(z_0, z_0) - r_0^3\mathbf{X}^4(z_0, z_0) + \dots \quad (8)$$

It is obvious from equations (7b) and (8) that no model of the subsurface is used in this procedure. Only the seismic data after deconvolution for the source wavefield, i.e. $\mathbf{X}(z_0, z_0)$ and the free surface reflectivity properties, the scalar r_0, are used. In fact, the data itself is used as the multiple prediction operator. Apparently, the data contains all necessary information about the subsurface to predict the multiples!

Note the fact that to eliminate the multiples of one shot record (one column in $\mathbf{X}(z_0, z_0)$], all other shot records [i.e., all other columns of the matrix $\mathbf{X}(z_0, z_0)$] are needed; the matrix multiplications describe 2-D convolutions of the data with itself in the time and space direction.

Avoiding temporal wraparound problems

Each matrix multiplication in the multiple elimination method of equation (7) or (8) will increase the traveltimes. The wraparound in the time domain can only be avoided by padding zeroes in the time direction before going to the frequency domain. However, this would mean that for eliminating Nth-order multiples the trace length should be roughly N times as long as the original length. This inconvenience can be overcome if the method is applied in the *complex* frequency plane (in fact in the Laplace domain). This can be achieved by applying a temporal taper of $\exp(-\alpha t)$ on the data, with α being a constant between 1 and 2. This exponential tapering procedure has been used in the past for modeling data in the frequency domain and is described in Rosenbaum (1974) and reviewed in Thybo (1989). After tapering, the data is Fourier transformed, and the multiple elimination method can be applied. The result is transformed back to the time domain, and the exponential taper is removed from the traces.

Adaptive multiple elimination

Using the data as a multiple prediction operator, requires that the data be properly deconvolved for the source wavefield and that the data have true amplitudes (both relative *and* absolute: the data should be a true unit-valued impulse response of the medium). Therefore, the procedure, as stated in equation (8), will never work satisfactorily on real data: an *adaptive* multiple elimination procedure must be implemented.

Substituting equations (1) and (3b) into equation (8) results in:

$$\mathbf{P}_0^-(z_0) = \mathbf{P}^-(z_0) - r_0\{\mathbf{P}^-(z_0)\mathbf{S}^+(z_0)^{-1}\}\mathbf{P}^-(z_0) + r_0^2\{\mathbf{P}^-(z_0)\mathbf{S}^+(z_0)^{-1}\}^2\mathbf{P}^-(z_0) - r_0^3\{\mathbf{P}^-(z_0)\mathbf{S}^+(z_0)^{-1}\}^3\mathbf{P}^-(z_0) + \dots \quad (9)$$

Assume for the moment that the source wavefield can be written as:

$$\mathbf{S}^+(z_0) = S(\omega)\mathbf{I}, \quad (10)$$

with $S(\omega)$ as the frequency-dependent source signature. This means that the assumption is made that an angle-dependent deconvolution for the source directivity pattern has been applied in advance, and that the residual sources consist of identical point sources each with signature $S(\omega)$. Note that a diagonal source matrix as defined in equation (10), implies pressure dipole sources, as explained in Berkhout (1982). To do the angle-dependent deconvolution, a forward description of the seismic source array should be calculated first. This array response can then be corrected for by a directional deconvolution procedure on common receiver gathers in the x-ω domain. Fokkema et al. (1990) describes such a directional deconvolution method in the x-ω domain. The deconvolution can also be applied in the k_x-ω or t-p domain if the plane layer assumption is valid. It can be argued that in many practical situations directional deconvolution can be omitted.

Using equation (10), equation (9) becomes:

$$\mathbf{P}_0^-(z_0) = \mathbf{P}^-(z_0) - A(\omega)[\mathbf{P}^-(z_0)]^2 + A^2(\omega)[\mathbf{P}^-(z_0)]^3 - A^3(\omega)[\mathbf{P}^-(z_0)]^4 + \dots, \quad (11a)$$

with surface factor

$$A(\omega) = r_0 S^{-1}(\omega). \quad (11b)$$

Note that equation (11a) includes matrix multiplications of the data with itself, showing that the result for one trace (matrix element) is constructed by a summation of contributions of a common receiver gather (row) with a common source gather (column). It corresponds to a Kirchhoff summation of the data extrapolated recursively with an operator, which is the data itself again (i.e., lateral convolutions).

The source signature $S(\omega)$ must also contain the scaling factor of the data and a possible time delay in the data. The factor $A(\omega)$ should scale (i.e., deconvolve) the terms $\mathbf{P}^-(z_0)^2$, $\mathbf{P}^-(z_0)^3$, etc., in such a way that the predicted multiples match in *amplitude and phase* with the multiples present in the data, so that they can be subtracted as shown in equation (11a).

As the frequency-dependent scaling factor $A(\omega)$, as defined in equation (11b), will generally not be known, it should be estimated by making the multiple elimination procedure adaptive in the sense that those values for $A(\omega)$ are to be found which give the best elimination of the multiples. The adaptive version is visualized in Figure 3. As a result, those optimal values of $A(\omega)$ give an estimate for the *inverse* of the source signature. Hence, by applying our adaptive multiple elimination process, the multiples are eliminated *and* the inverse source signature in the data is estimated at the same time! This estimated inverse source signature can be used to deconvolve the source signature. Note that r_0 and $S^{-1}(\omega)$ cannot be estimated independently, but only in combination, i.e., $A(\omega)$ is estimated. Note also that $A(\omega)$ contains any amplitude and phase information of the recording instrument and the preprocessing algorithm.

Using equation (11) for multiple elimination on single-component land data, we assume an average (angle-independent) free-surface reflection coefficient r_0 instead of a reflectivity matrix $\mathbf{R}^-(z_0)$. If we know the reflection characteristics of the free surface for land data (from the velocities just below the free surface), it is, of course, possible to take this into account by calculating the terms $\underline{\mathbf{R}}^-(z_0)\underline{\mathbf{P}}^-(z_0)^2$, $\{\underline{\mathbf{R}}^-(z_0)\underline{\mathbf{P}}^-(z_0)\}^2\underline{\mathbf{P}}^-(z_0)$, etc., [as in equation (7)] to estimate the inverse source signature. Note that what is estimated is the *original* source signature that has been emitted by the source, which is not identical to the *wavelet* you see on your traces.

To judge whether the multiples have been eliminated, the total energy in the resulting upgoing wavefield is used. We assume that, after having eliminated all surface-related multiples, a minimum energy is contained in the upgoing wavefield. This is intuitively understood by considering the fact that the free surface bounces the upgoing energy back into the medium, causing an increase of energy. Note that in equation (11a), the first term (the data $\underline{\mathbf{P}}^-(z_0)$ itself) is not affected by $A(\omega)$. This means that the primaries are preserved during the optimization procedure. After optimization, the estimated function $A(\omega)$ can be used to deconvolve the primary data set for further processing steps.

For the optimization process, $A(\omega)$ is parametrized by a number of definition points in the frequency domain, and the complete function is interpolated (see Figure 3). This is done to keep the number of parameters low. Taking a coarse sampling in the frequency domain, for example Δf, also has the advantage in that the time length of the estimated inverse source signature is limited to $1/\Delta f$. The interpolation procedure can be applied, e.g., by a Fourier-based sinc-interpolation or by a cubic spline interpolation. The actual optimization can be done by any standard technique. For the examples discussed in this paper, a steepest descent method has been used.

Note that the terms $\underline{\mathbf{P}}^-(z_0)^2$, $\underline{\mathbf{P}}^-(z_0)^3$, etc., can be calculated in advance. The residual energy is a function of the frequency-dependent scaling function $A(\omega)$ only, as can be observed in equation (11a). Therefore, during the optimization process, only a weighted summation of these terms has to be applied for each new set of parameters [see equation 11(a)]. Note also that no assumption on the source signature need be made (zero phase or minimum phase), which means that *any* mixed phase source signature can be estimated!

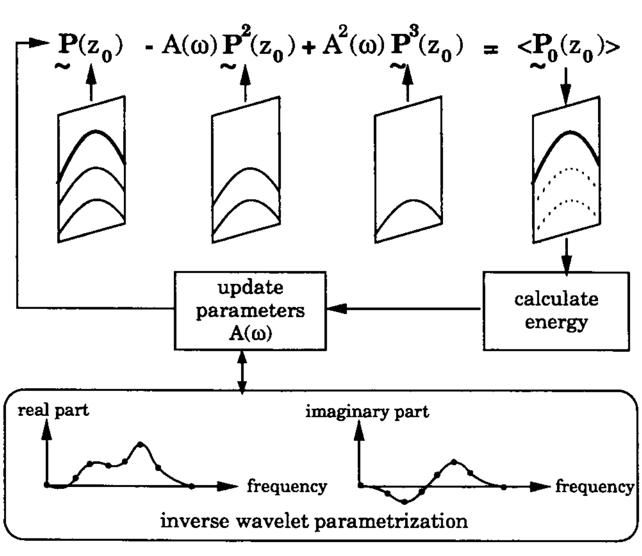

FIG. 3. Adaptive multiple elimination, simultaneously estimating of the source signature by minimizing the total energy in the data. (Note that the matrices represent all shot records in the frequency domain and the data panels represent one shot record in the time domain).

Decomposition of single-component data

In the preceding sections, the input for the multiple elimination procedure were supposed to represent the *upgoing* pressure wavefield $\underline{\mathbf{P}}^-(z_0)$ *at* the free surface. Both for marine and land data this is not the actual measured data. In the case of marine data, the *total* pressure is measured *below* the free surface, whereas for land data the vertical component of the *total* particle velocity is measured at the free surface. So before starting the multiple elimination process, decomposition should be applied to arrive at upgoing reflected wavefields due to downgoing source wavefields. This type of decomposition is generally referred to as "deghosting."

First we consider the marine data case. The receivers are located at depth level z_d below the free surface and detect the total pressure wavefield. For one monochromatic shot record, the recorded wavefield is written as $\mathbf{P}(z_d)$, which is one column of the data matrix $\underline{\mathbf{P}}(z_d)$ for the frequency component under consideration. If the free surface can be locally considered as flat and the medium near the surface as locally homogeneous, the decomposition process can be carried out in the k_x-ω domain. In this domain, we have $\tilde{P}(k_x, z_d, \omega)$, i.e., $\mathbf{P}(z_d)$ after a Fourier transform in the x-direction, which is the sum of the upgoing wavefield $\tilde{P}^-(k_x, z_d, \omega)$ and the downgoing wavefield $\tilde{P}^+(k_x, z_d, \omega)$ after reflection against the free surface (the ghost). Using the phase shift operator for propagation we obtain

$$\tilde{P}(k_x, z_d, \omega) = \tilde{P}^-(k_x, z_d, \omega) + \tilde{P}^+(k_x, z_d, \omega) = \tilde{P}^-(k_x, z_d, \omega)[1 + r_0 e^{-2jk_z\Delta z}], \quad (12)$$

with $k_z = \sqrt{k^2 - k_x^2}$, $k = \omega/c = 2\pi f/c$, f is the frequency, c the P-wave velocity in water and $\Delta z = |z_d - z_0|$. Inverting equation (12) yields the upgoing wavefield at depth level $z = z_d$. Extrapolating this wavefield up to the free surface results in:

$$\tilde{P}^-(z_0) = \frac{e^{-jk_z\Delta z}}{1 + r_0 e^{-2jk_z\Delta z}} \tilde{P}(z_d). \quad (13)$$

Equation (13) describes the acoustic decomposition procedure, which removes the receiver ghost as a function of angle and extrapolates the ghost-free upgoing wavefield to $z = z_0$. To reduce instabilities, stabilizing equation (13) is recommended by applying a high-angle reduction filter and adding a stabilization factor ε to the denominator ($\varepsilon \approx 0.01$).

For the source ghost, a similar decomposition could be applied, but if the source depth is rather small (smaller than half the dominant wavelength) a monopole source, together with its ghost, form a dipole source. Since the adaptive multiple elimination procedure, as described by equation (11), assumes dipole sources [see equation (10)], the source ghost should be left unharmed. As mentioned before, if high angle multiple energy needs to be removed, the directivity effect of source and receiver arrays should be removed by deconvolution.

For land data, the vertical component of the particle velocity of the wavefield at the free surface is recorded.

Wapenaar and Berkhout (1989) give the relation in the k_x-ω domain between the total pressure $\tilde{P}(k_x, z, \omega)$ and the vertical velocity component $\tilde{V}_z(k_x, z, \omega)$ at a depth level z, as well as the up- and downgoing pressure wavefields $\tilde{P}^-(k_x, z, \omega)$ and $\tilde{P}^+(k_x, z, \omega)$:

$$\begin{bmatrix} \tilde{P}^+(k_x, z, \omega) \\ \tilde{P}^-(k_x, z, \omega) \end{bmatrix} = \frac{1}{2} \begin{bmatrix} 1 & \dfrac{\omega\rho}{k_z} \\ 1 & \dfrac{-\omega\rho}{k_z} \end{bmatrix} \begin{bmatrix} \tilde{P}(k_x, z, \omega) \\ \tilde{V}_z(k_x, z, \omega) \end{bmatrix}, \quad (14)$$

where ρ is the local density of the medium. At the free surface $z = z_0$, the total pressure $\tilde{P}(k_x, z_0, \omega)$ vanishes, hence,

$$\tilde{P}^-(k_x, z_0, \omega) = -\frac{1}{2}\frac{\omega\rho}{k_z}\tilde{V}_z(k_x, z_0, \omega). \quad (15)$$

For land data stabilization, adding a small positive number to the denominator of equation (15) is needed to avoid dividing by zero. Of course, the treatment of land data can only be completely satisfactory if multicomponent data is available. Equation (15) refers to P-waves only.

On land, the surface medium parameters may vary laterally, meaning that the decomposition operators should be calculated with the *local* parameters. Transforming the operators from the k_x-ω domain to the x-ω domain yields different spatial deconvolution operators for different lateral positions. These can be stored in the columns of a decomposition matrix and applied to the data by a matrix multiplication.

Examples of single-component multiple elimination

To illustrate our method, we first consider a horizontally layered model, allowing an instructive qualitative and quantitative discussion. Figure 4a gives the velocity and density log as a function of two-way traveltime. Figure 4b shows a shot record modeled in this medium using an acoustic finite-difference modeling algorithm. The trace sampling is 12.5 m and the number of offsets shown is 300. Both source and receivers were positioned 5 m below the free surface. The source is a monopole and the receivers measure the total pressure wavefield. Figure 6a shows the mixed-phase source signature used for this modeling. The first processing step is a decomposition of the recorded wavefield into the upgoing wavefield at the free surface. The result of this procedure for the shot record of Figure 4b is shown in Figure 5a. The effect of this decomposition is twofold: it restores the original source signature from ghost interference, and it restores the amplitude versus offset from the angle dependent character of the receiver ghost. Next, the adaptive surface-related multiple elimination process is applied to the data of Figure 5a. We see in Figure 5b that all 10 primaries can be easily identified (which is impossible in Figure 5a) and that only minor internal multiples remain in the lower part of the section. The results of the multiple elimination process can also be verified from the velocity panels corresponding to the sections of Figure 5a and 5b. Figure 6b shows the estimated source signature, which is almost identical to the original source signature within the frequency band of estimation (six definition points between 8 and 48 Hz). As expected, it is impossible to recover the source signature up to 80 Hz, as the energy is very low above 50 Hz. Note that the phase spectrum has also been accurately recov-

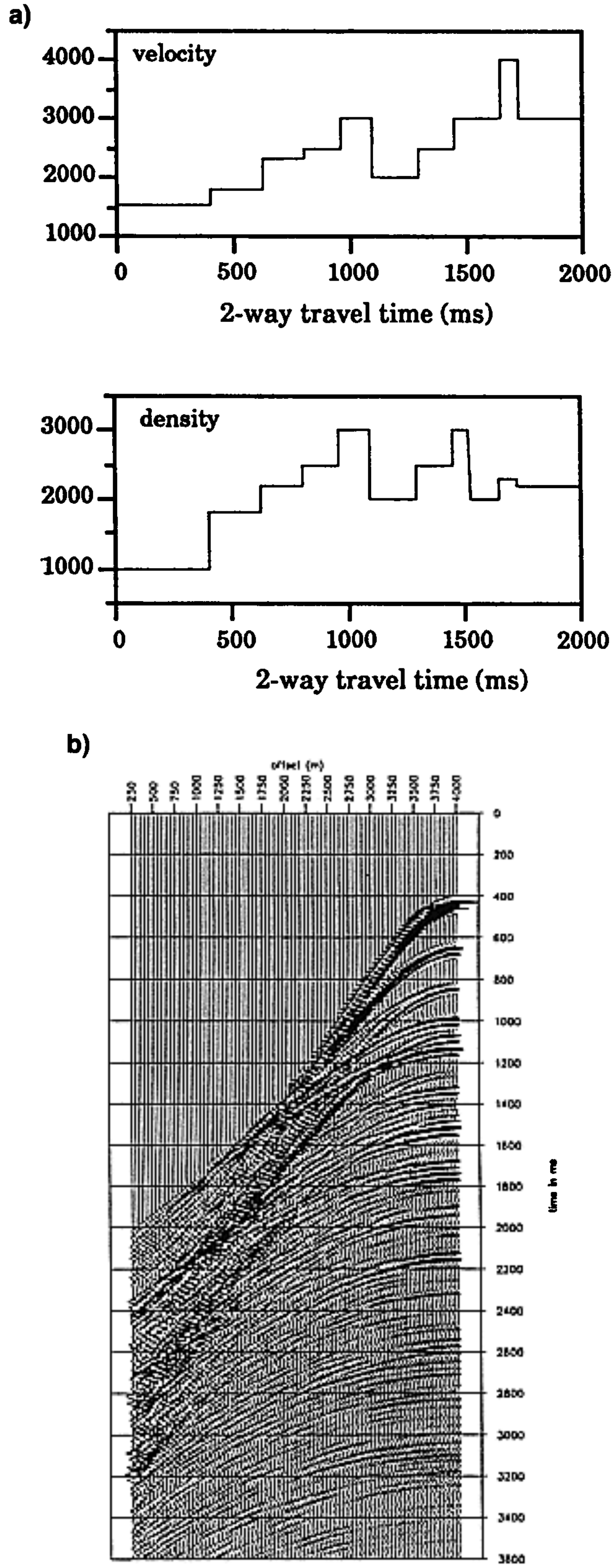

FIG. 4. (a) A horizontally layered medium used to model seismic data with acoustic "finite-difference" software. The velocity and density logs are given as a function of two-way traveltime. (b) Realistically simulated shot record in the subsurface model of (a). The data shown represent the total wavefield measured just below the free surface.

ered without making any assumption. The initial guess for the steepest descent optimization was a spike signature.

Next, we examine the subsurface model of Figure 7. It contains strong lateral inhomogeneities with a dome structure. Note that the model is not completely symmetric around the dome structure. Figure 8a shows a shot record after modeling with an acoustic finite-difference algorithm with the source at 1100 m, which is just to the left of the top of the dome. As can be observed from Figure 8a, the multiples have a very complex behavior and a very high amplitude compared to the primaries of the deeper interfaces. After adaptive surface-related multiple elimination, the result for the shot record of Figure 8a is shown in Figure 8b. The strong multiples (indicated in Figure 8a) have been eliminated and the weak primaries (indicated in Figure 8b) have been very well restored from interference with the multiples. Figure 8c and d show the zero offset section of this data set before and after multiple elimination. Note the diffractions that are visible in the curved part of the first reflection; they are true primaries due to the model discretization; the resulting complex "stair case" reflectivity behavior of the first interface could be fully handled by the multiple elimination scheme (we do not need any subsurface information). Note also, that for the multiple elimination result of one shot record, all other shot records are involved. This can be understood from the multiplication of the data matrix with itself, where rows (common receiver gathers) are multiplied with columns (common shot gathers).

MULTIPLE ELIMINATION FOR MULTICOMPONENT DATA

Due to the fact that we use the matrix notation, the surface-related multiple elimination method can easily be extended to multicomponent land data. It only requires extension of the matrix notation such that each matrix element becomes a subvector. For an elaborate description of the multicomponent matrix notation see Wapenaar et al. (1990).

Using the multicomponent data and the elastic description of the free surface reflectivity, it is possible to remove all surface-related multiples *and* conversions from the data. We have obtained excellent results on synthetic land data. The next step will be an evaluation on field data.

EXAMPLE ON A REAL MARINE DATA SET

The acoustic multiple elimination process, consisting of about 300 shot records with 120 traces each, has been applied to marine data. The source and receiver spacing is 25 m. The missing near-offset gap is 150 m. If these offsets are left empty, serious edge effects will contaminate the multiple elimination result. Hence, the missing offsets have been interpolated. In the figures, the interpolated traces are deleted. Figure 9a shows the result of the adaptive multiple elimination process for one shot gather (shot 180) with, from left to right, the shot gather with multiples, the shot gather after multiple elimination and the difference between them, i.e., the eliminated multiples. Figure 9b shows the velocity panels belonging to the same shot position for the data with and without multiples and the multiples only. Both from Figure 9a and b it is clear that the multiple elimination worked very well and that primaries could be separated from the multiples. Also note the enormous amount of multiple energy compared to the primary energy (see at arrows). The velocity panels show that all eliminated events are (correlated) multiple events indeed. Note again that for the result on one shot gather all other shots

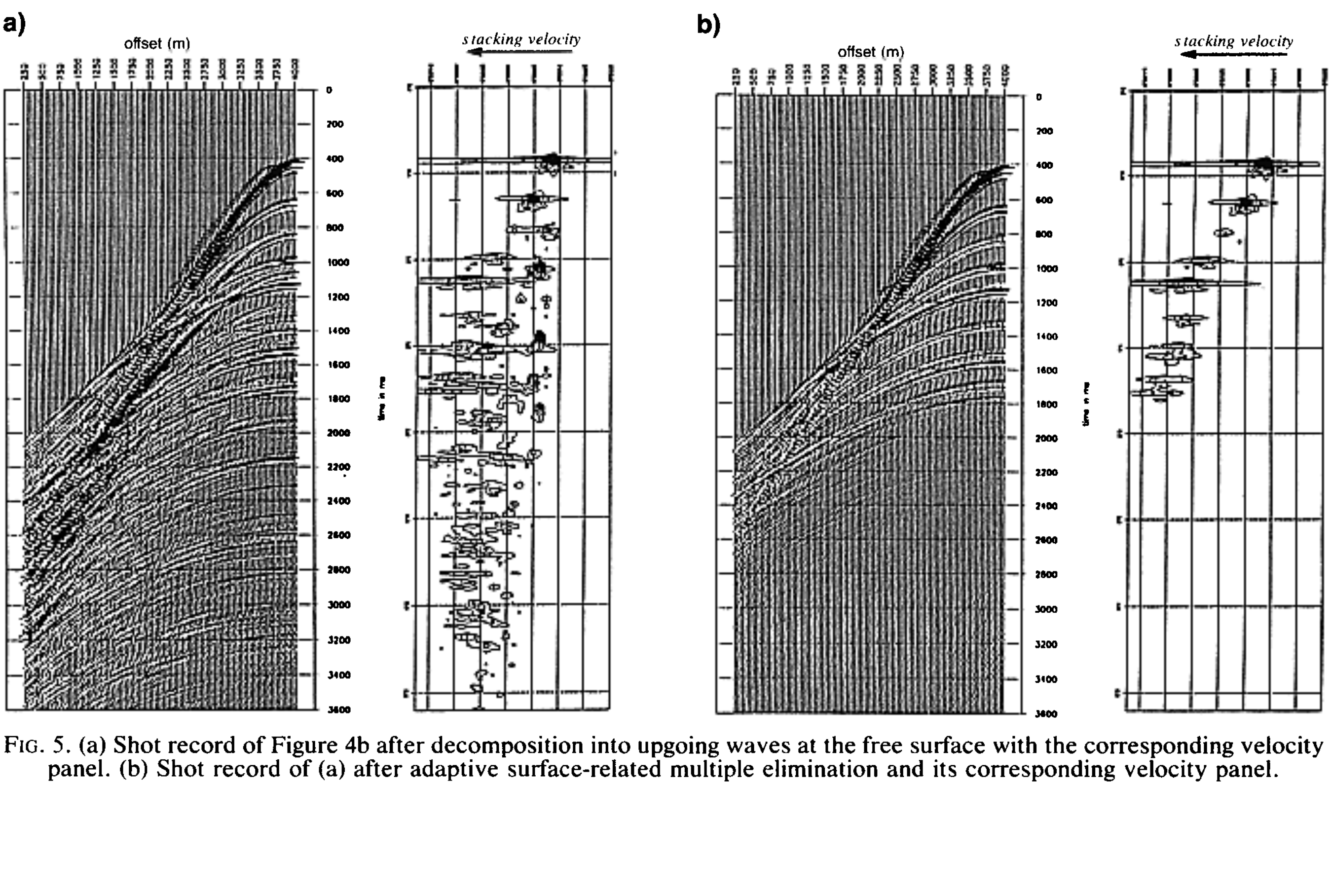

FIG. 5. (a) Shot record of Figure 4b after decomposition into upgoing waves at the free surface with the corresponding velocity panel. (b) Shot record of (a) after adaptive surface-related multiple elimination and its corresponding velocity panel.

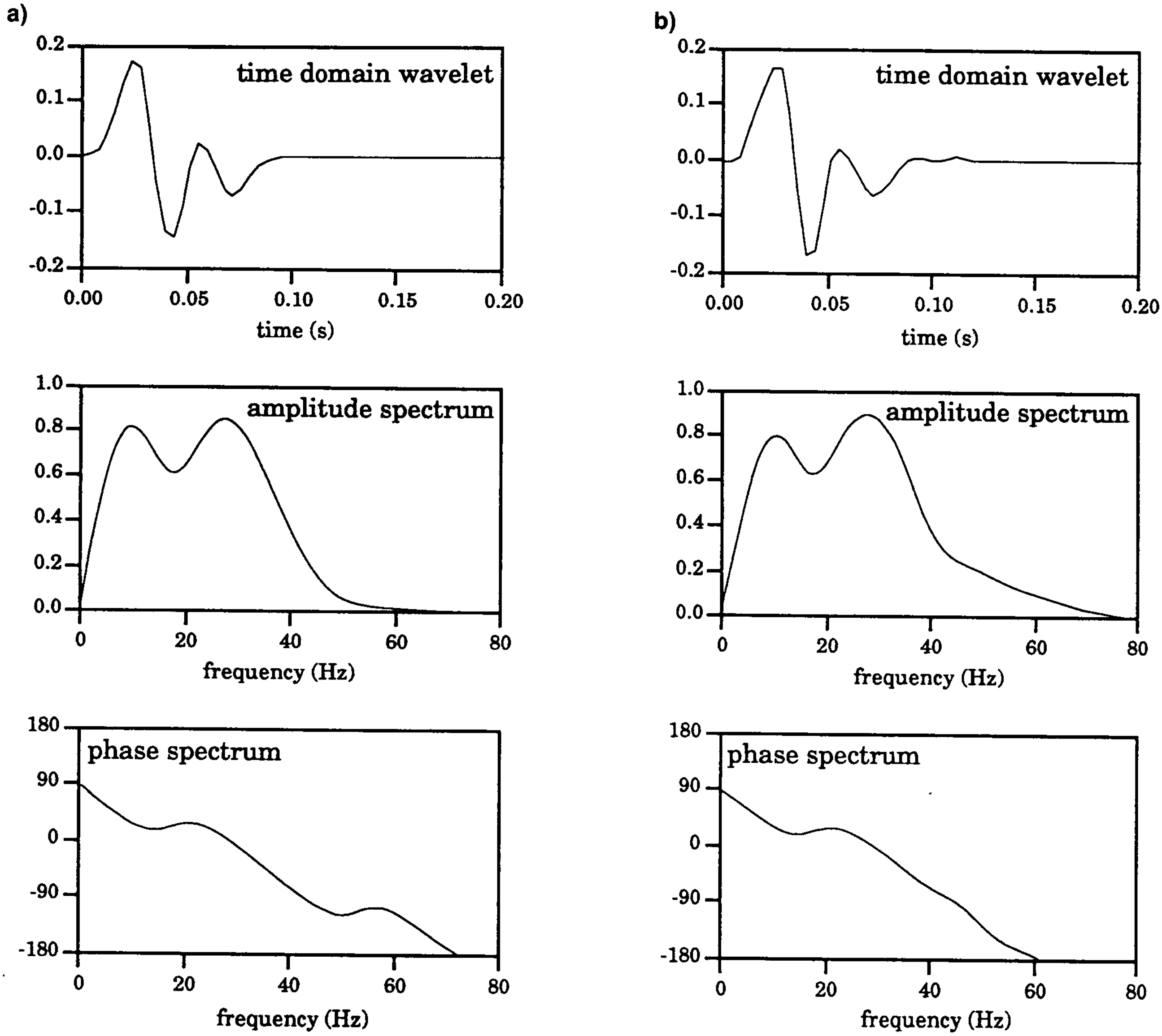

FIG. 6. (a) Mixed phase source signature used to model the shot record of Figure 4b. (b) Estimated source signature after the adaptive multiple elimination. The phase spectra are plotted after a shift of the signature of −24 ms.

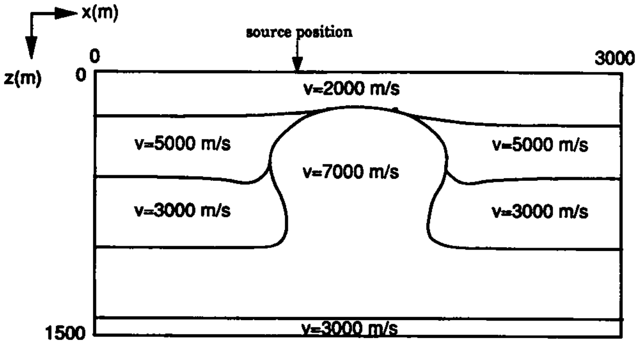

FIG. 7. Subsurface model with a dome for modeling seismic data.

were also used; the information to predict multiples for one shot record is distributed over all other shot records.

The multiple elimination method took approximately 10 minutes of CPU time per shot record on a Convex C1 and 30 seconds of CPU time per shot record on a Cray YMP. The algorithm has not been fully optimized for speed.

A common offset section from the data before and after multiple elimination has been selected, which is shown in Figure 10a and b, respectively. In these sections, we can observe the varying character of multiples going from left to right. Small disturbances in subsurface reflectivity produce large variations in multiple energy. Note especially the small synclinal structure in the sea bottom around shot 70, which produces a focusing effect of multiples. The result of this lateral inhomogeneity in the subsurface on the multiples could be handled perfectly with our scheme as no assumptions on the subsurface have to be made. Figure 10c shows the difference plot of the sections before and after multiple elimination; it shows the large amount of removed multiple energy.

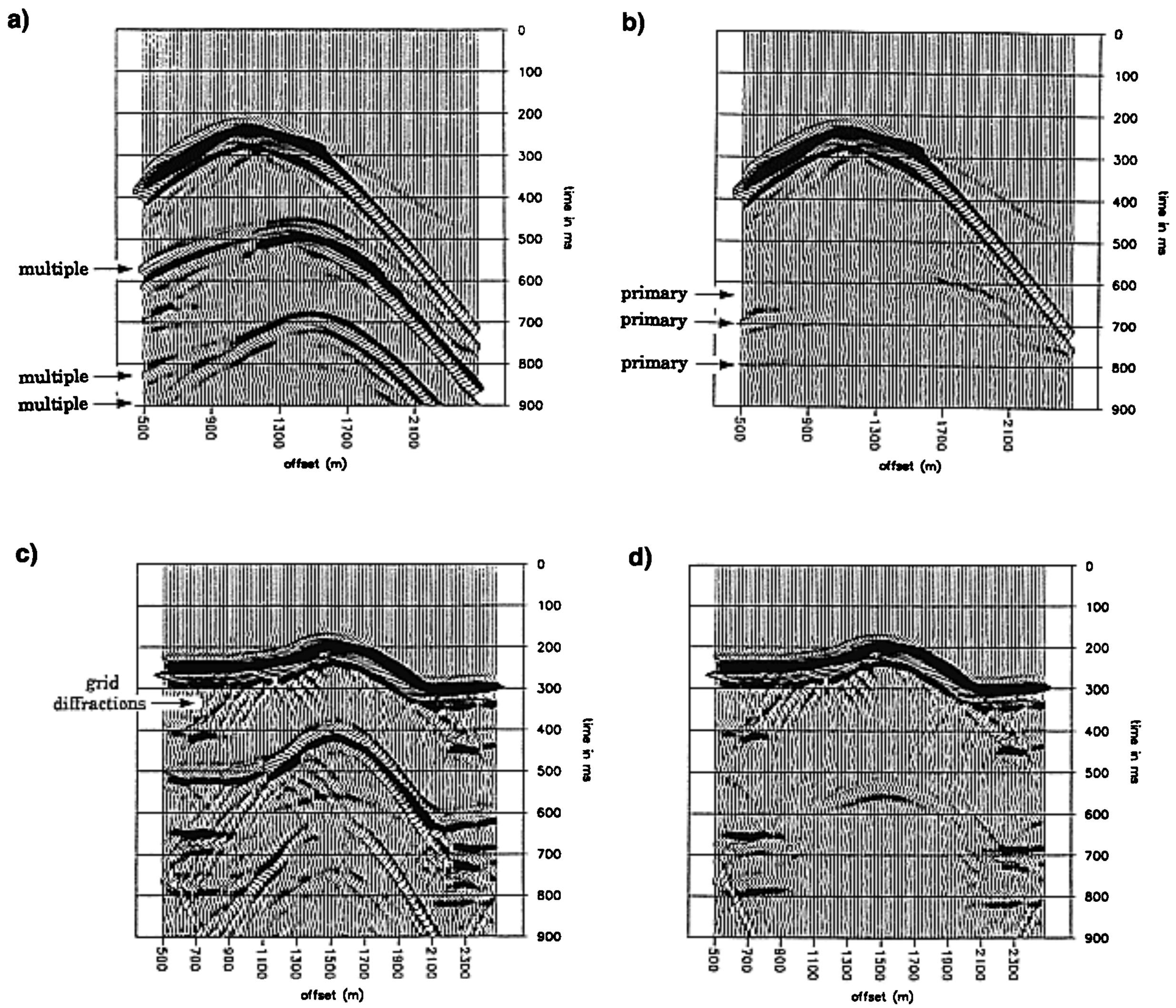

FIG. 8. (a) Shot record with source at 1100 m. in the model of Figure 7. (b) Same shot record after adaptive surface-related multiple elimination. (c) Zero offset section from the data modeled in the subsurface model of Figure 7. (d) Zero offset section after adaptive surface-related multiple elimination.

Also, a stack of the data has been generated before and after multiple elimination; the velocity analysis was done on the data *after* multiple elimination. Figure 11a shows the stacking result with multiples. As expected, the removal of multiple energy is not so spectacular on the stacked sections, because for this situation the velocity differences between primary and multiple events is sufficient to remove a significant amount of multiple energy by stacking. But there are still many multiples that appear on the stack before multiple elimination (Figure 11a) which have been effectively removed by the surface-related multiple elimination method (Figure 11b). In Figure 11a, some of these events and areas have been indicated by arrows. As a matter of fact, these are the multiples that have small moveout differences with the primaries and belong to the category "remaining surface-related multiples." To judge the value of the stack after multiple elimination, the difference plot of the stacked section before and after surface-related multiple elimination is shown in Figure 11c. The difference plot shows correlated events, especially in the lower part of the section. In the target zone, which is between 2200 and 2400 ms, a stacked multiple of 2300 ms is visible at the left side of Figure 11c (see the arrow); it is masking the primary reflection that occurs at the same time in Figure 11b. Note again the band of focused multiples under the small synclinal structure around CMP positions 70 and 170 in Figure 11c. As a last remark on this subject, it should be mentioned that the improvement of prestack data (restoring the primaries over the full offset range (see Figure 9a) is of more interest to the industry than the improvement of the stack.

Finally, Figure 12 shows the estimated source signature from this marine data set. We allowed a small noncausal part for this source signature because the seismic data has been band-pass filtered with a zero phase filter. Note that no assumption was used on the property of the phase spectrum.

EXTENSIONS OF THE MULTIPLE ELIMINATION METHOD

Inversion of the multiple response

After the multiple elimination method, we end up with:

1) the primary section (with internal multiples);
2) an estimated (inverse) source signature;
3) the multiple section.

In conventional inversion, the primary data are used as input. However, as the proposed processing method provides the multiple response as well, we are now working on a

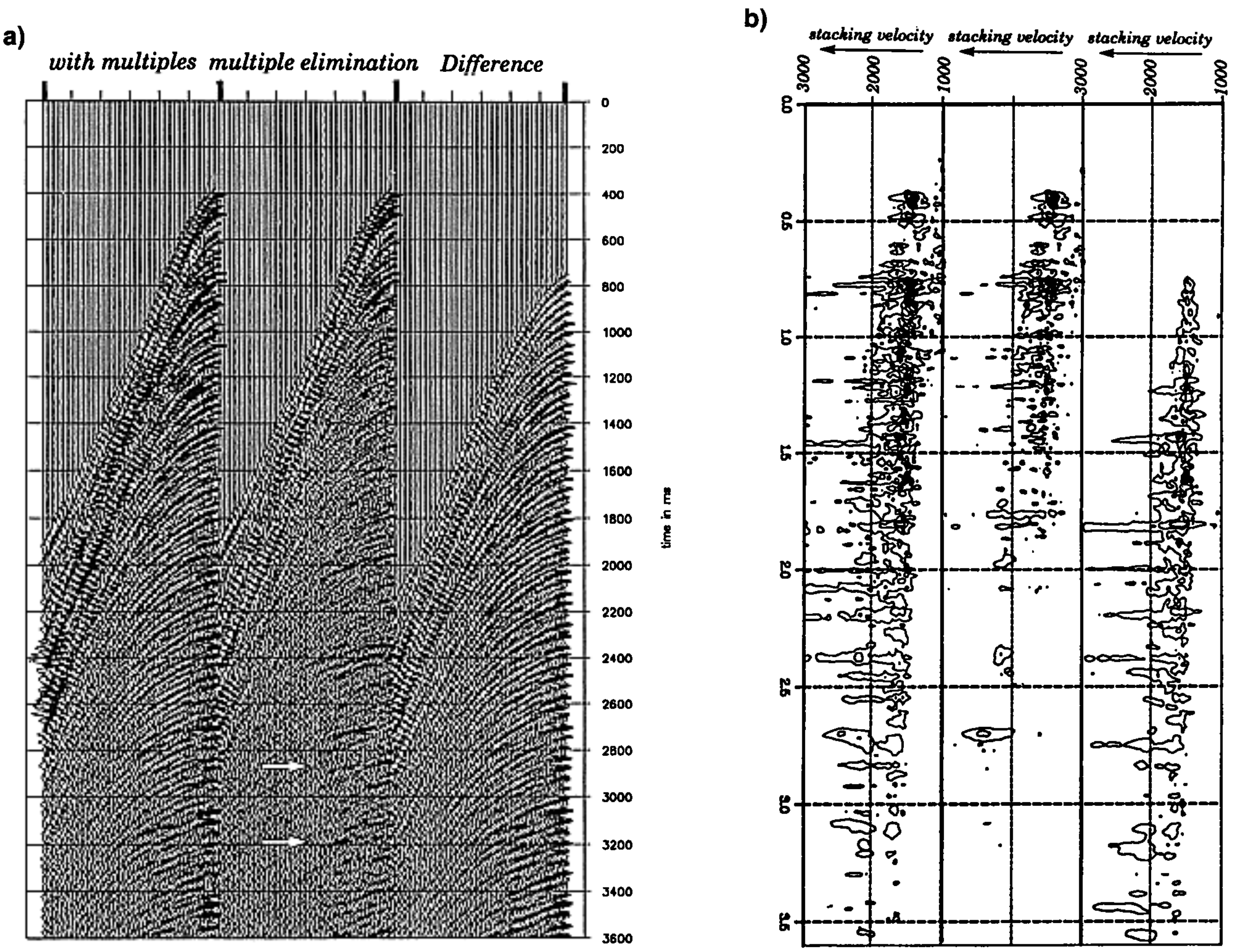

FIG. 9. Shot record of real data set. (Courtesy SAGA Petroleum A.S.) (a) Shot record before multiple elimination, after multiple elimination and the difference between them, i.e., the eliminated multiples. (b) The velocity panels belonging to the sections of (a).

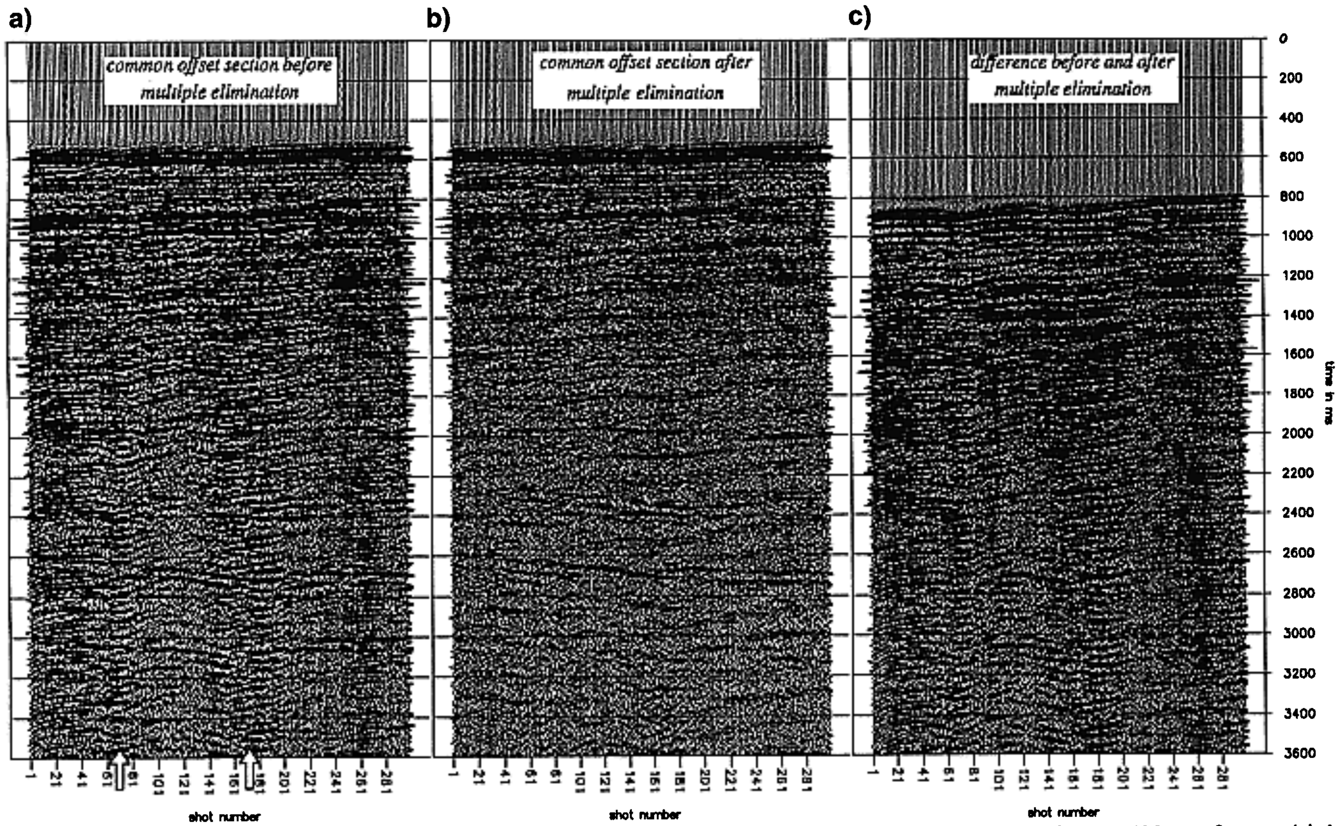

FIG. 10. (a) Common offset section of 600 m before multiple elimination. (b) Common offset section at 600 m after multiple elimination. (c) Difference plot of the common offset sections before and after multiple elimination.

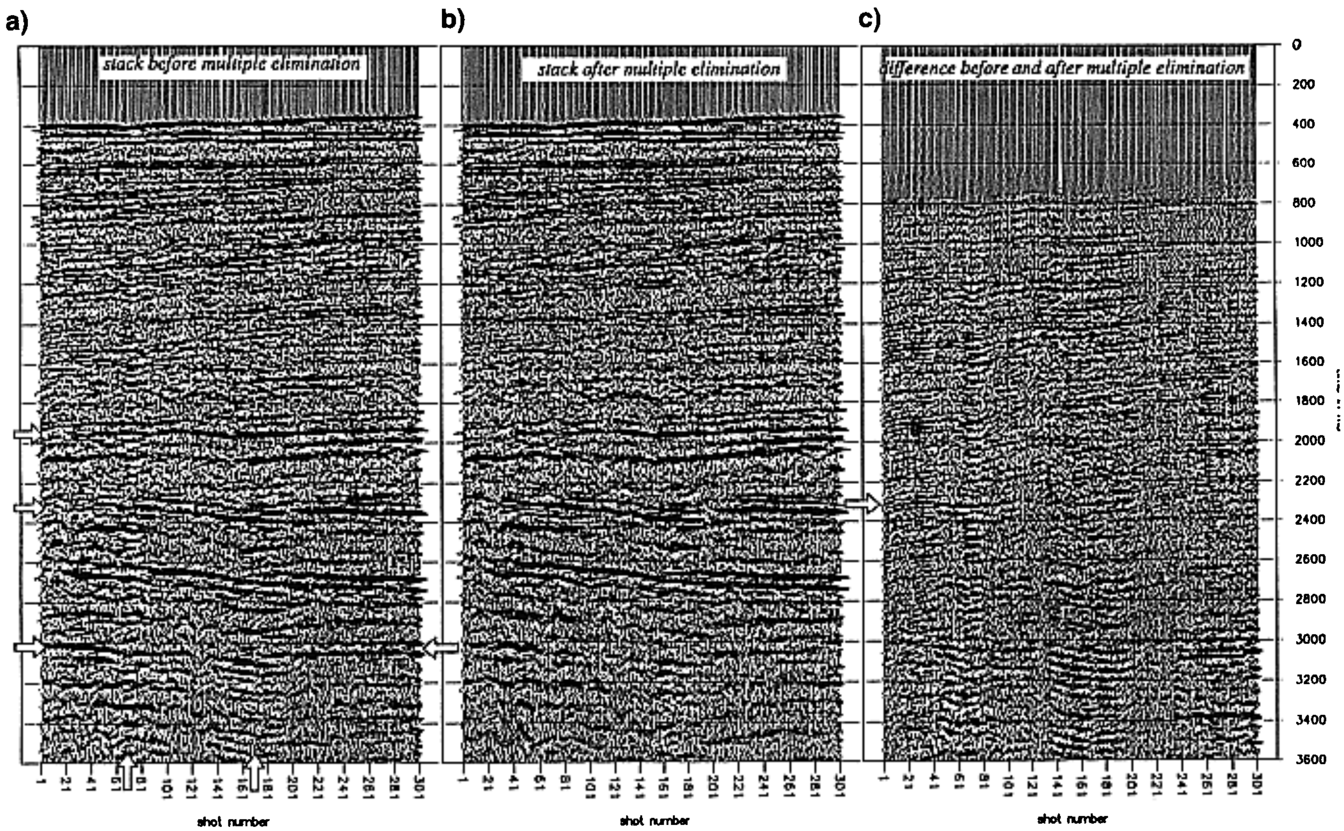

FIG. 11. (a) Stacked section before multiple elimination. (b) Stacked section of the data after multiple elimination. (c) Difference plot of the stacked sections before and after multiple elimination.

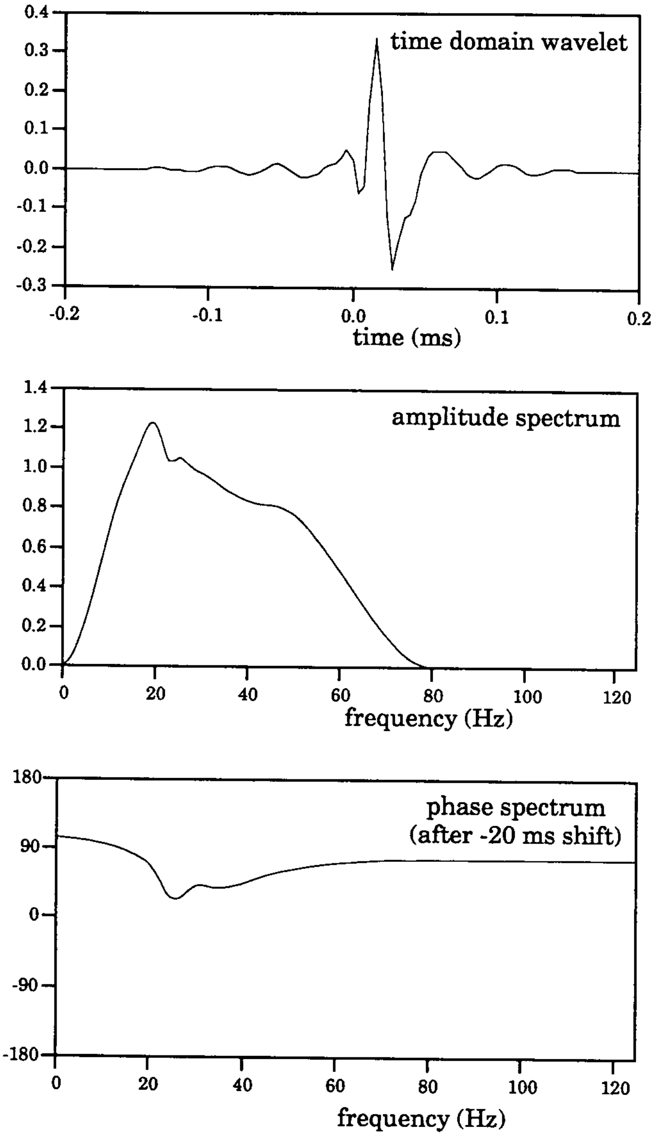

FIG. 12. Estimated signature from the real marine data set.

complementary inversion scheme that uses the multiple data as input. As the multiple data contains more information on the multiple-generating boundaries than the primary data, it may be expected that the complementary inversion scheme will be pre-eminently suited to estimate the upper part of the surface.

Applying the multiple elimination method recursively for internal multiples

After multiple elimination, the "primary" data can be downward extrapolated to a new "surface" and the adaptive multiple elimination process can be applied again with respect to the new surface. Actually, this process could be made part of prestack depth migration: e.g., internal multiples are removed after applying the imaging principle and before applying the next extrapolation step (Berkhout, 1982, chapter 7).

Those extensions are currently being implemented.

CONCLUSIONS

A prestack inversion method has been proposed that removes all surface-related multiples without any knowledge about the subsurface. Data from any inhomogeneous medium can be handled. If multicomponent data is available, all surface-related conversions can be removed as well, taking the elastic reflectivity effect of the free surface into account. Before the multiple elimination process can be applied, the source wavefield together with the data scaling factor and the surface reflectivity must be known (surface-related parameters). Because the source wavefield (with scaling factor) is not available in practice, the proposed process must be applied adaptively, estimating the scaled source signature by minimizing the energy in the data after multiple elimination. Hence, together with the properly scaled multiple free data, an estimate of the source signature is obtained as well! Another unique property of the proposed method is that primaries and multiples may have exactly the same moveout. Results on simulated data and on field data show that the proposed multiple elimination process may become one of the key inversion steps in stepwise seismic inversion (Berkhout and Wapenaar, 1990).

ACKNOWLEDGMENTS

The authors would like to thank the Dutch Technology Foundation (S.T.W.) and the sponsors of the DELPHI consortium for their financial support. In addition, the authors are grateful to SAGA Petroleum A.S. for providing the field data set.

REFERENCES

Anstey, N. A., and Newman, P., 1967, Part I: The sectional auto-correlogram and Part II: The sectional retro-correlogram: Geophys. Prosp., **14**, 391–426.

Berkhout, A. J., 1982, Seismic migration: Imaging of acoustic energy by wavefield extrapolation. A. Theoretical aspects, second edition: Elsevier Science Publ. Co., Inc., 211–218.

Berkhout, A. J., and Wapenaar, C. P. A., 1990, Delphi: Delft philosophy on acoustic and elastic inversion, part 1: The Leading Edge, **9**, no. 2, 30–33.

Bernth, H., and Sonneland, L., 1983, Wavefield extrapolation techniques for prestack attenuation of water reverberations: 53rd Ann. Internat. Mtg., Soc. Explo. Geophys., Expanded Abstracts, 264–265.

Berryhill, J. R., and Kim, Y. C., 1986, Deep-water peg-legs and multiples: emulation and suppression, Geophysics, Volume 51, 2177–2184.

Fokkema, J. T., Baeten, G. J. M., and Vaage, S., 1990, Directional deconvolution in the F-X domain: 60th Ann. Internat. Mtg., Soc. Explo. Geophys., Expanded Abstracts, 1673–1676.

Kennett, B. L. N., 1979, The suppression of surface multiples on seismic records, Geophys. Prosp., **27**, 584–600.

Rosenbaum, J. M., 1974, Synthetic microseismograms: Logging in porous formations: Geophysics, **39**, 14–32.

Thybo, H., 1989, Wraparound removel from one-dimensional synthetic seismograms: Geophysics, **54**, 911–915.

Verschuur, D. J., Berkhout, A. J., and Wapenaar, C. P. A., 1989, Wavelet estimation by prestack multiple elimination: 59th Ann. Internat. Mtg., Soc. Explo. Geophys., Expanded Abstracts, 1129–1132.

Wapenaar, C. P. A., and Berkhout, A. J., 1989, Elastic wavefield extrapolation: Redatuming of single- and multi-component seismic data: Elsevier Science Publ. Co., Inc.

Wapenaar, C. P. A., Herrmann, P., Verschuur, D. J., and Berkhout, A. J., 1990, Decomposition of multi-component seismic data into primary *P*- and *S*-wave responses, Geophys. Prosp., **38**, 633–661.

Wiggins, J. W., 1988, Attenuation of complex water-bottom multiples by wave-equation based prediction and subtraction: Geophysics, **53**, 1527–1539.